Comparison of poly(ethylene glycol)-based networks obtained by cationic ring opening polymerization of neutral and 1,2,3-triazolium diepoxy monomers

Antoine Jourdain, Mona M Obadia, Jannick Duchet-Rumeau, Julien Julien Bernard, Anatoli Serghei, François Tournilhac, Jean-Pierre Pascault, Eric Drockenmuller

Cross–linked Solid Electrolyte Obtained by Cationic Ring Opening Polymerization of a Diepoxy 1,2,3–Triazolium Ionic Liquid

Antoine Jourdain,[a,b] Mona M. Obadia,[a] Jannick Duchet–Rumeau,[b] Julien Bernard,[b] Anatoli Serghei,[a] François Tournilhac,[c] Jean–Pierre Pascault,[b] and Eric Drockenmuller[a,*]

[a)] *Univ Lyon, Université Lyon 1, CNRS, Ingénierie des Matériaux Polymères, UMR 5223, F–69003, Lyon, France*

[b)] *Univ Lyon, INSA Lyon, CNRS, Ingénierie des Matériaux Polymères, UMR 5223, F–69003, Lyon, France*

[c)] *Molecular, Macromolecular Chemistry, and Materials, ESPCI Paris, PSL Research University, 10 Rue Vauquelin, F–75005 Paris, France*

ABSTRACT: Poly(1,2,3–triazolium)s are a versatile class of poly(ionic liquid)s that take advantage of the functional tolerance, orthogonal robustness and efficiency of the copper(I)–catalyzed azide–alkyne cycloaddition (CuAAC). We use this reaction to design an all-in-one monomer gathering polymerization, crosslinking and ion-conducting functionalities in a single small molecule. A diepoxy 1,2,3–triazolium (DET) ionic liquid monomer is synthetized by CuAAC ligation between alkyne– and azide–functionalized epoxies, followed by *N*–alkylation of the central 1,2,3–triazole group by *N*–methyl bis(trifluoromethylsulfonyl)imide. Advantageously, this monomer is a low viscosity liquid which can therefore be implemented by casting. As a mode of curing, we chose cationic homopolymerization in bulk to obtain readily a network without dilution by a comonomer nor release of byproducts. Two cross–linked epoxy networks were thereby obtained i) from DET and ii) from a commercial poly(ethylene glycol) diglycidyl ether (PEGDGE, M_n = 500 g mol^{-1}), taken as a neutral reference monomer, using

benzylamine trifluoroborate as cationic initiator. The polymerization kinetics and the structure/properties correlations of the resulting ionic and neutral epoxy networks are discussed based on differential scanning calorimetry, thermogravimetric analysis and swelling/extractible measurements, as well as thermomechanical properties obtained by torsional rheometry and ionic conductivity measured by broadband dielectric spectroscopy. Although the ionic epoxy network exhibits a lower cross–link density (i.e. higher swelling ratio and lower storage modulus in the rubber state) than the neutral network due to the more pronounced occurrence of transfer and termination reactions, this work demonstrates that cationic ROP is a suitable route to produce a network solely from 1,2,3 triazolium functionalized diepoxy monomer.

KEYWORDS: Poly(ionic liquid)s, 1,2,3–Triazoliums, Click chemistry, Epoxy networks, Cationic ring opening polymerization.

INTRODUCTION

Poly(ionic liquid)s (PILs) ideally combine the best features of ILs (e.g. tunable solubility, enhanced thermal and (electro)chemical stability as well as ion conducting properties, etc.) with those of polymer materials (e.g. processability, viscoelasticity, adhesion, film–forming and mechanical properties, tunable microstructure, etc.).[1–4] Polymerization of IL monomers (ILMs) or post–polymerization chemical modification of neutral polymers has enabled the access to a broad range of PILs assembled from a wide library of cations (e.g. ammonium, pyrrolidinium, imidazolium, phosphonium, 1,2,4– or 1,2,3–triazolium, etc.), anions (e.g. halides, inorganic fluorides, perfluorinated sulfonimides, etc.), and microstructures (e.g. block copolymers, (hyper)branched polymers, colloids, self–assembled nanoparticles, surface–tethered polymer brushes, coatings, as well as chemical, physical and dynamic networks, etc.).[5–8] The application of different chain–growth or step–growth polymerization methods has afforded a broad variety of PILs (e.g. styrenics, (meth)acrylates, vinyl esters, *N*–vinyl– and *C*–vinyl–imidazoliums, polyesters, polyimides, polyurethanes, etc.). Shortly after their introduction in 2013, 1,2,3–triazolium–based PILs (TPILs) have been established as a structurally rich family of PILs with performances reaching those of the best PILs developped so far.[3] Their synthesis merges the versatility of different step growth or chain growth polymerization methods with the functional tolerance of CuAAC, together with the quantitative nature of 1,2,3–triazoles *N*–alkylation reaction and optional ion metathesis. A broad library of TPILs with tailored structure, functionality and properties, e.g. linear and hyperbranched ionenes,[9,10] poly(meth)acrylates,[11,12] polystyrenes,[13] poly(vinyl ester)s,[14] poly(4–vinyl–1,2,3–triazolium)s,[15] poly(ethylene glycol)s,[16] poly(aryl ether)s,[17] polyurethanes,[18] polypeptoids,[19] or polysiloxanes,[20] has been developed using robust, efficient and orthogonal synthetic approaches.

Numerous reports have already demonstrated the potential of PILs in applications including catalysis,[21,22] dye–sensitized solar cells,[23] electrochromic devices,[24,25] gas separation membranes,[26,27] antimicrobial surfaces,[28] sensors and actuators,[29,30] electrolyte–gated transistors,[31] fuel cells,[32] as well as

devices for energy storage such as batteries or super–capacitors.[33–36] Most of these applications rely on PILs having enhanced ion conducting properties generally in the form of highly viscous liquids. Several strategies have been developed to yield mechanically stable PIL–based solid electrolytes. A convenient approach involves the dispersion of molecular ILs within thermoplastic or thermosetting matrices.[27,32,37] However, the synthesis of chemically cross–linked PILs having one of the ionic moieties covalently attached to the polymer network are of particular interest since they prevent phase separation upon aging and afford enhanced mechanical properties. Typical examples of the most common synthetic pathways to achieve the synthesis of PIL networks include the chain–growth polymerization of difunctional ILMs,[38] the chain–growth copolymerization of an ILM with either a neutral or an IL difunctional monomer,[39] the step–growth polymerization of a difunctional ILM with a multifunctional neutral monomer (e.g. epoxy amine polyaddition, etc.),[40] as well as the post–polymerization chemical cross–linking of multifunctional PIL intermediates.[41]

Herein, we explore the ring opening polymerization (ROP) of a synthetic diepoxy 1,2,3–triazolium (DET) ILM as a new approach to provide cross–linked solid polymer electrolytes. We detail (i) the synthesis of DET ILM; (ii) the comparison of two anionic and two cationic initiators for the ROP of DET using DSC and FTIR; (iii) the measurement of the activation energy of the systems by DSC, the investigation of polymerization kinetics using FTIR and DSC, and the evolution of the glass transition temperature with conversion for DET and a neutral diepoxy monomer (PEGDGE) by DSC; (iv) the gelation behavior of both epoxy systems by rheology and DSC experiments; and (v) the investigation of structure/properties correlations by TGA, DSC, swelling experiments, torsional rheometry and broadband dielectric spectroscopy for both types of epoxy networks.

EXPERIMENTAL SECTION

Materials. Sodium hydride (NaH, 90%), epichlorohydrin (99.5%), *N*,*N*–diisopropylethylamine (DIPEA, 99%), iodo(triethyl phosphite)copper(I) ($CuP(OEt)_3I$, 97%), *N*–methyl bis(trifluoromethylsulfonyl)imide (**4**, CH_3TFSI, 90%), methylimidazole (1–MI, 99%), 2–phenylimidazole (2–PI, 98%) and poly(ethylene glycol) diglycidyl ether (**6**, PEGDGE, M_n = 500 g mol^{-1}) were purchased from Aldrich and used as received. 2–(2–(2–(Prop–2–ynyloxy)ethoxy)ethoxy)ethanol **1**,[42] 2–(2–(2–(2–azido–ethoxy)–ethoxy)–ethoxymethyl)–oxirane **3**,[43] 4–chloroaniline trifluoroborate ($4CA–BF_3$),[44] and benzylamine trifluoroborate ($BzA–BF_3$),[45] were synthesized as described previously.

Nuclear Magnetic Resonance. ^1H (400 MHz) and ^{13}C (100 MHz) NMR spectra were recorded on a Bruker Avance 400 spectrometer in $CDCl_3$ using residual hydrogenated solvent peak as reference (δ7.26). Abbreviations for peak multiplicity are s for singlet, d for doublet, dd for doublet of doublet, t for triplet and m for multiplet.

Thermal Characterizations. DSC was performed using a DSC Q200 (TA Instrument) calibrated with an indium standard. The samples were prepared using hermetic pans and the experiments were conducted under a helium purge of 25 mL min^{-1} at a heating rate of 10 °C min^{-1}. Thermogravimetric analysis (TGA) was performed using a TGA Q500 (TA Instruments). A heating ramp from 20 to 600 °C was applied at 10 °C min^{-1} under a helium purge of 60 mL min^{-1} to ca. 8 mg of epoxy networks **7** or **8**.

DSC Monitoring of the Curing Process. Initially, several DSC capsules containing ca. 5 mg of reactive mixture of diepoxy monomers **5** or **6** with BzA–BF_3 (0.075 mol EE^{-1}) were sealed off under ambient conditions and heated in the DSC apparatus from –100 to 200 °C at a heating rate of 10 °C min^{-1} to obtain the initial glass transition temperature (T_{g0}), the initial differential heat capacity (ΔC_{p0}) and the total enthalpy of reaction (ΔH_{∞}). Following each initial scan, a second dynamic scan from –100 to 200 °C at 10 °C min^{-1} was performed to evaluate the final glass transition temperature ($T_{g\infty}$) and the final differential heat capacity ($\Delta C_{p\infty}$) of the resulting network. T_g values were taken as the midpoint of the heat capacity change. T_{g0}, T_g, ΔC_{p0} and $\Delta C_{p\infty}$ values are average values obtained from 5 different runs. In addition, several capsules were heated in an oven at 130 °C for reaction times ranging from 10 to 350 min before being quenched in liquid nitrogen and directly analyzed by DSC to access $T_{g(t)}$ of the formed epoxy network and residual enthalpy of reaction, $\Delta H_{(t)}$. The conversion of reactive groups (x) at a given time t is given by equation 1:

$$x = 1 - \frac{\Delta H_{(t)}}{\Delta H_{\infty}} \quad (1)$$

IR Monitoring of the Curing Process. Isothermal curing processes were monitored using a Bruker–Tensor 37 IR spectrometer at a resolution of 4 cm^{-1}, equipped with a thermally controlled SPECAC Goldengate ATR accessory. A mixture of DET **5** or PEGDGE **6** with BzA–BF_3 (0.075 mol EE^{-1}) were deposited on the ATR diamond in the center of a Teflon seal covered with a metallic lid held in place by pressure, resulting in a leak–proof cavity presenting very good atmosphere tightness. Transmitted $I(\nu)$ and incident $I_0(\nu)$ beam energies were converted into a spectrum in absorbance A using the ATR correction: $A(\nu) = -(\nu/1000) \times \log[I(\nu)/I_0(\nu)]$ where ν is the wavenumber in cm^{-1}. The disappearance of the absorption peak at 914 cm^{-1} (epoxy bending) was monitored to determine the conversion of epoxy groups (α_{epoxy}) using equation (2):

$$\alpha_{epoxy} = 1 - \left(\frac{A^t_{914}}{A^0_{914}}\right) \quad (2)$$

with A_{914}^{0} and A_{914}^{t} the absorbance of epoxy groups before and after curing for a reaction time *t*, respectively.

Water Content Measurement by Karl–Fischer Titration. Titration of water content in diepoxy monomers **5** and **6** was carried out by Karl–Fischer method on a 917 Coulometer apparatus from Metrohm. This apparatus is associated to an oven 860 KF Thermoprep where 50 mg of monomers **5** or **6** are melted at 160 °C.

Rheology Monitoring of the Curing Process. Reactive mixtures of diepoxy monomers **5** or **6** (3.00 g, 3.90 mmol of **5** or 6.00 mmol of **6**) with BzA–BF_3 (0.075 mol EE^{-1}) were placed at 130 °C in the gap of an Anton Paar Physica MCR 501 rheometer equipped with 50 mm diameter disposable parallel plates. *G*' and *G*" data were collected every 20 s for a frequency of 1 rad s^{-1} and an amplitude of 5%. Gel time (t_{gel}) was taken as the crossing time of *G*' and *G*".

Broadband Dielectric Spectroscopy. The ionic conductivity of epoxy networks **7** and **8** was measured by Broadband Dielectric Spectroscopy (BDS) using a high resolution Alpha–Analyzer (Novocontrol GmbH) assisted by a Quatro temperature controller. A solution of 200 mg of DET **5** or PEGDGE **6** with BzA–BF_3 (0.075 mol EE^{-1}) in acetone (0.5 mL) was casted onto a platinum electrode (3 cm in diameter) and the solvent was slowly evaporated for ca. 1 h under ambient conditions. The sample was cured during 10 h at 110 °C, and then under vacuum for 10 h at 110 °C and 3 h at 130 °C. A second platinum electrode (2 cm in diameter) was then placed on top of the sample to build up a measurement cell in a parallel plate configuration. A further annealing under nitrogen during 3 h at 110 °C was performed in the cryostat of the dielectric spectrometer while continuously monitoring the complex conductivity function

$$\sigma^*(\omega,T) = \sigma'(\omega,T) + i\sigma''(\omega,T) \quad (3)$$

Ionic conductivity measurements were started once a constant value of $\sigma^*(\omega,T)$ was attained, affording thus well equilibrated anhydrous samples. Then, the complex conductivity function was measured under isothermal conditions at temperatures ranging from 110 to −50 °C each 10 °C by applying frequency

sweeps from 10 MHz to 0.1 Hz and a voltage of 0.1 V. The low value of applied voltage excludes any possible non–linear effects that can take place at the interface with the measurement electrodes. The temperature was controlled by heating the sample under a flow of pure nitrogen, which excluded the presence of oxygen and moisture in the measurement chamber. The thermal stability was set to be better than 0.1 K in absolute values with relative variations less than 0.2 K min^{-1}. After completing the measurements several temperature points were re–measured to ensure that the experimental results were stable and reproducible.

Swelling Experiments. Epoxy networks were immersed in acetone at room temperature for 48 h. The swollen mass was obtained by measuring the weight after immersion. The samples were then dried under vacuum at 50 °C until a stable dry weight was reached. The swelling ratio (*S*) and the amount of extractibles (*X*) were calculated using Equations 4 and 5:

$$S = \frac{(m_{wet} - m_{dry})}{m_{dry}} \quad (4)$$

$$X = \left(1 - \left(\frac{m_{dry}}{m_0}\right)\right) \times 100 \quad (5)$$

with m_0, m_{wet}, and m_{dry} the initial mass, the swollen mass and the mass after drying of the networks, respectively.

Thermomechanical Properties. Temperature sweep experiments were performed on a strain–controlled ARES G2 rheometer (TA instruments) using rectangular samples (20 × 5 × 2 mm^3) in torsion mode at a frequency of 1 Hz in the linear viscoelastic domain. The applied heating rate was 3 °C min^{-1} for temperatures ranging from −80 to 100 °C.

Synthesis of 2–2–(2–(2–prop–2–ynyloxy–ethoxy–ethoxy)–ethoxymethyl)–oxirane 2. NaH (2.37 g, 98.8 mmol) was added in small portions to a solution of 2–(2–(2–(prop–2–ynyloxy)ethoxy)ethoxy)ethanol (7.43 g, 39.5 mmol) in anhydrous THF (150 mL) maintained at 0 °C under argon. The mixture was brought to room temperature and stirred for 45 min before adding epichlorohydrin (7.7 mL, 99 mmol) and further stirring under argon for 18 h. After neutralization of

residual NaH by ethanol (20 mL), water (50 mL) was added and THF was evaporated under reduced pressure. The mixture was extracted with dichloromethane (3 × 150 mL). After drying the combined organic layers by $MgSO_4$ and evaporation of the solvents, the crude product was purified by column chromatography on silica gel eluting with a 3:2 mixture of petroleum ether and ethyl acetate to afford **2** as a colorless liquid (6.84 g, 71.0%). ^{1}H NMR ($CDCl_3$, 400 MHz): δ 4.14 (2H, d, J = 2.4 Hz, H_f), 3.73 (1H, dd, J = 3.2, 12.0 Hz, H_c), 3.60 (12H, m, H_d, H_e), 3.37 (1H, dd, J_1 = 6.0 Hz, J_2 = 11.6 Hz, $H_{c'}$), 3.10 (1H, m, H_b), 2.73 (1H, dd, J = 4.4, 5.2 Hz, H_a), 2.55 (1H, dd, J = 2.8, 5.2 Hz, $H_{a'}$), 2.40 (1H, t, J = 2.4 Hz, H_h). ^{13}C NMR ($CDCl_3$, 100 MHz): δ 79.46 (1C, C_h), 74.42 (1C, C_g), 71.77 (1C, C_c), 70.67,70.55,70.35 (5C, C_d), 68.89 (1C, C_e), 58.19 (1C, C_f), 50.62 (1C, C_b), 44.05 (1C, C_a). HRMS (ESI) m/z: $[M+Na]^+$ calcd for $C_{12}H_{20}NaO_5$, 267.1203; found, 267.1198.

Synthesis of Diepoxy 1,2,3–Triazole 3. $CuP(OEt)_3I$ (0.35 g, 0.99 mmol) was added to a solution of **1** (4.00 g, 19.8 mmol), 2–(2–(2–(2–azido–ethoxy)–ethoxy)–ethoxymethyl)–oxirane **2** (4.26 g, 19.8 mmol), and DIPEA (2.56 g, 19.8 mmol) in THF (50 mL) that was stirred for 16 h at 60 °C. The solvent was evaporated under vacuum and the crude product was purified by column chromatography on silica gel eluting with a 3:2 mixture of petroleum ether and ethyl acetate to afford after evaporation of the solvents **3** as a slightly yellow liquid (4.57 g, 55.4%). ^{1}H NMR ($CDCl_3$, 400 MHz): δ 7.69 (1H, s, H_g), 4.60 (2H, s, H_i), 4.47 (2H, t, J = 5.2 Hz, H_f), 3.81 (2H, t, J = 5.2 Hz, H_e), 3.76–3.68 (2H, m, H_c, H_k), 3.67–3.47 (20H, m, H_d, H_j), 3.39–3.27 (2H, m, $H_{c'}$, $H_{k'}$), 3.13–3.03 (2H, m, H_b, H_l), 2.77–2.67 (2H, m, H_a, H_m), 2.57–2.47 (2H, m, $H_{a'}$, $H_{m'}$). ^{13}C NMR ($CDCl_3$, 100 MHz): δ 144.68 (1C, C_h), 123.61 (1C, C_g), 71.76 (2C, C_c, C_k), 70.83–70.22 (10C, C_d, C_j), 67.41 (1C, C_e), 64.36 (1C, C_i), 50.58 (2C, C_b, C_l), 49.99 (1C, C_f), 43.96 (2C, C_a, C_m). HRMS (ESI) m/z: $[M+H]^+$ calcd for $C_{21}H_{38}N_3O_9$, 476.2603; found, 476.2594.

Synthesis of Diepoxy 1,2,3–Triazolium 5. A solution of 1,2,3–triazole **3** (1.00 g, 2.40 mmol) and CH_3TFSI **4** (1.06 g, 3.60 mmol) in acetonitrile (10 mL) was stirred for 24 h at 70 °C. CH_3CN and the excess of CH_3TFSI were then evaporated under vacuum and the crude product was purified by column chromatography on silica gel eluting with a 4:1 mixture of ethyl acetate and methanol to afford, after evaporation of the solvents, **5** as a brown liquid (1.70 g, 99.6%). ^{1}H NMR ($CDCl_3$, 400 MHz): δ 8.57 (1H, s, H_g), 4.81 (2H, s, H_i), 4.71 (2H, t, *J* = 4.8 Hz, H_f), 4.29 (3H, s, H_n), 3.96 (2H, t, *J* = 4.8 Hz, H_e), 3.83–3.74 (2H, m, H_c, H_k), 3.74–3.52 (20H, m, H_d, H_j), 3.34–3.25 (2H, m, $H_{c'}$, $H_{k'}$), 3.14–3.05 (2H, m, H_b, H_l), 2.78–2.70 (2H, m, H_a, H_m), 2.60–2.50 (2H, m, $H_{a'}$, $H_{m'}$). ^{13}C NMR ($CDCl_3$, 100 MHz): δ 140.39 (1C, C_h), 130.16 (1C, C_g), 119.71 (2C, q, *J* = 319.0 Hz, C_o), 71.92 (2C, C_c, C_k), 70.78–69.89 (10C, C_d, C_j), 67.47 (1C, C_e), 60.23 (1C, C_i), 53.80 (1C, C_f), 50.68 (2C, C_b, C_l), 43.97 (2C, C_a, C_m), 38.44 (1C, C_n). HRMS (ESI) m/z: $[M]^+$ calcd for $C_{22}H_{40}N_3O_9$, 490.2759; found, 490.2748. $[M]^-$ calcd for $C_2F_6NO_4S_2$, 279.9178; found, 279.9166.

General Procedure for the Preparation of Epoxy Networks. Synthesis of 7. Diepoxy 1,2,3–triazolium **5** (5.00 g, 6.49 mmol) and BzA–BF_3 (0.17 g, 0.97 mmol, 0.075 mol EE^{-1}) were dissolved in acetone (5 mL). Acetone was then evaporated under reduced pressure for 6 h at room temperature. The resulting homogeneous mixture was introduced in 5.1 × 2.3 × 1.3 cm^3 silicone molds and was sequentially cured under vacuum for 2 h at 100 °C, 8 h at 130 °C and 1 hour at 150 °C to afford ca. 2 mm thick ionic epoxy network **7** as a flexible brown solid. The same procedure was applied for the preparation of neutral epoxy network **8** using PEGDGE **6** (5.06 g, 10.1 mmol), BzA–BF_3 (263 mg, 1.50 mmol, , 0.075 mol EE^{-1}) and acetone (5 mL).

Scheme 1. Synthesis of Diepoxy 1,2,3–Triazolium 5

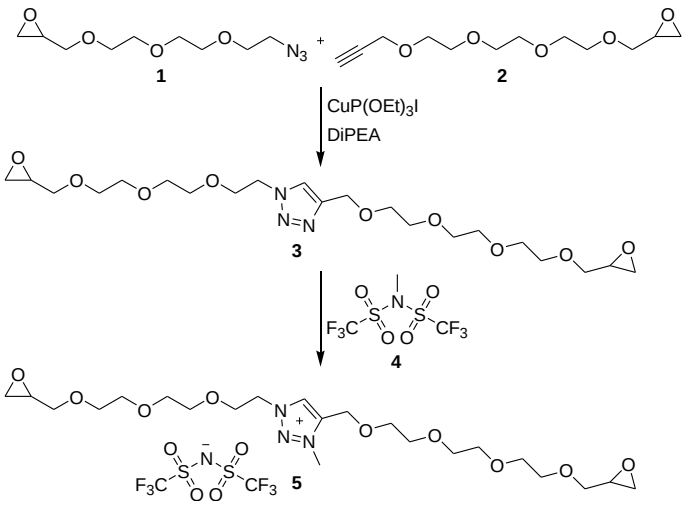

RESULTS and DISCUSSION

Synthesis of Diepoxy 1,2,3–Triazolium 5. In order to achieve the synthesis of ionic epoxy networks by ROP we have developed a novel multistep synthetic strategy affording a diepoxy–functionalized ILM having a central 1,2,3–triazolium cation, a TFSI counter–anion and two terminal epoxy groups (**Scheme 1**). Compared to previously reported diepoxy–functionalized 1,2,3–triazolium ILM that contained ester linkages and aliphatic spacers at the *N*–1 and *C*–4 positions,[46] DET **5** contains ether linkages and longer triethylene glycol–based spacers separating the terminal epoxy moieties from the central 1,2,3–triazolium group. Azide–functionalized epoxide **1** was synthesized in two–steps by azidation of 2–(2–(2–chloro–ethoxy)–ethoxy)–ethanol and subsequent *O*–Alkylation of the resulting azido–alcohol with epichlorohydrin.[42] Alkyne–functionalized epoxide **2** was synthetized by *O*–alkylation of 2–(2–(2–(prop–2–ynyloxy)ethoxy)ethoxy)ethanol with epichlorohydrin. Complementary epoxy–functionalized azide **1** and alkyne **2** were then coupled by CuAAC to afford after purification by column chromatography diepoxy 1,2,3–triazole (DET) **3** in 55% yield. Finally, *N*–alkylation at the *N*–3 position of the 1,2,3–triazole group of **3** using CH_3TFSI **4** afforded DET **5** in quantitative yield, after evaporation of the solvent and excess CH_3TFSI **4**. The purity of compounds **2**, **3** and **5** was demonstrated by ^{1}H and ^{13}C NMR spectroscopy (**Figures S1–S6**) and by electrospray ionization high–resolution mass spectroscopy

(ESI–HRMS). However, DSC monitoring of the curing of crude DET **5** (**Figure S7**) shows an exotherm starting at 160 °C most likely corresponding to the polymerization of epoxy groups initiated by traces of an unidentified inorganic impurity coming from CH_3TFSI **4**, a commercial reagent with 90% purity, that could not be detected by the employed analytical methods. Nevertheless, DET **5** was finally purified by column chromatography, a versatile and efficient purification method rarely used for the purification of ILs or ILMs, eluting with a 4:1 ethyl acetate/methanol mixture. After purification , DSC monitoring of purified DET **5** does not show any sign of reactivity up to 250 °C (**Figure S7**).

Investigation of Different Initiators for the Ring Opening Polymerization of DET 5. Epoxy monomers have gathered a lot of interest since their commercial introduction in 1947 as they rely on a unique versatile chemistry involving non–volatile intermediates, a wide range of curing temperatures, and low shrinkage during curing.[47] Epoxy networks exhibit a large range of properties suited for various applications such as composites, paints and varnishes, photoresists for microelectronics, and more recently 3D–printing.[48] Difunctional epoxy monomers can yield cross–linked networks either by step–growth polymerizations with comonomers such as diamines or by catalytic chain–growth ring opening polymerization or copolymerization with cyclic anhydrides. Although there has been a significant amount of work regarding the preparation of PIL–based cross–linked solid electrolytes by step–growth copolymerization of epoxy or diepoxy ILMs using the epoxy–amine reaction,[46,49–51] to the best of our knowledge neither the cationic nor the anionic ROPs of diepoxy ILMs have been investigated so far. The chain–growth ROP of diepoxy monomers can be mediated by anionic or cationic initiators[52] such as imidazoles,[53] Lewis acids such as BF_3 complexes,[44,45,54,55] or onium salts.[56,57]

Herein, we have initially investigated the ability of classical anionic and cationic initiators (**Scheme S1**) to promote the ROP of DET **5** by DSC monitoring of the total reaction enthalpy (ΔH_∞). Although being classical anionic initiators for the ROP of diepoxy monomers,[53] 1–methyl imidazole (1–MI) and 2–phenyl imidazole (2–PI) are not suited for the ROP of DET **5**. Indeed, for both anionic initiators at a

content of 0.075 mol EE^{-1} ΔH_∞ is below ca. 10 kJ EE^{-1} (**Figure S8**) while values of ca.100 kJ EE^{-1} are generally observed for the anionic ROP of classical diepoxy monomers.[58] For both initiators, the beginning of a second exotherm can be observed above 200 °C, a temperature too high to prevent degradation and spontaneous polymerization of epoxy groups. Besides, even after 15 h of curing at 135 °C the resulting materials can be dissolved in acetone attesting the poor efficiency of the anionic initiation for the ROP of DET **5** and the insufficient cross–link density of the resulting materials. This poor initiation observed for imidazole initiators might result from the trans-*N*-alkylation reaction between 1,2,3-triazoliums and imidazole which has been previously demonstrated to be reversible for 1,2,3-triazoliums while it is irreversible in the case of the resulting imidazoliums.[58]

Cationic ROP of DET **5** was then investigated using two classical cationic initiators for the ROP of diepoxy monomers, i.e. 4–chloroaniline trifluoroborate (4CA–BF_3),[54] and benzylamine trifluoroborate (BzA–BF_3).[45] DSC monitoring (**Figure S8**) shows that both initiators exhibit comparable reaction enthalpies (ΔH_∞ = 88 and 91 kJ EE^{-1} for 4CA–BF_3 and BzA–BF_3, respectively) thus confirming comparable and quantitative conversion of epoxy groups. However, while 4CA–BF_3 starts initiating the ROP of DET **5** near room temperature (onset temperature = 30 °C) which could complicate the handling and storage of reactive mixtures, BzA–BF_3 initiates the ROP at higher temperature (onset temperature = 85 °C) making it an ideal initiating system. Therefore, BzA–BF_3 (0.075 mol EE^{-1}) was chosen as cationic initiator for the further detailed study of the ROP of DET **5** (**Scheme 2**). Besides, the cationic ROP of PEGDGE **6** (M_n = 500 g mol^{-1}, X_n ~ 8, $Đ$ = 1.46), a commercially available neutral diepoxy monomer having both a molar mass and a number of ethylene glycol units comparable to the cationic moiety of DET **5**, was also investigated for comparison.

Scheme 2. Synthesis of Epoxy Networks 7 and 8 by Cationic ROP of DET 5 and PEGDGE 6 Initiated by BzA–BF_3

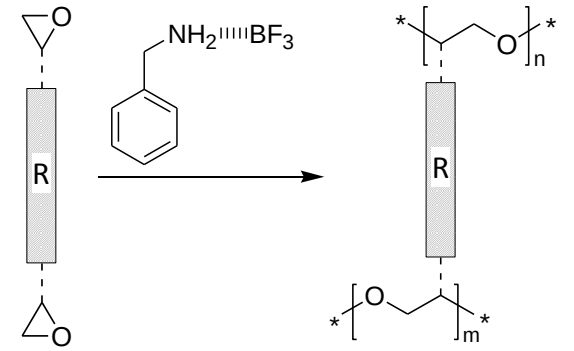

5,**7**: R =

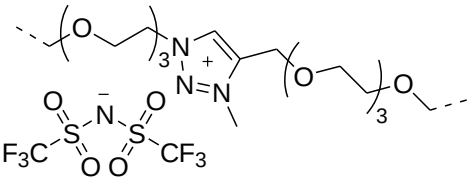

6,**8**: R =

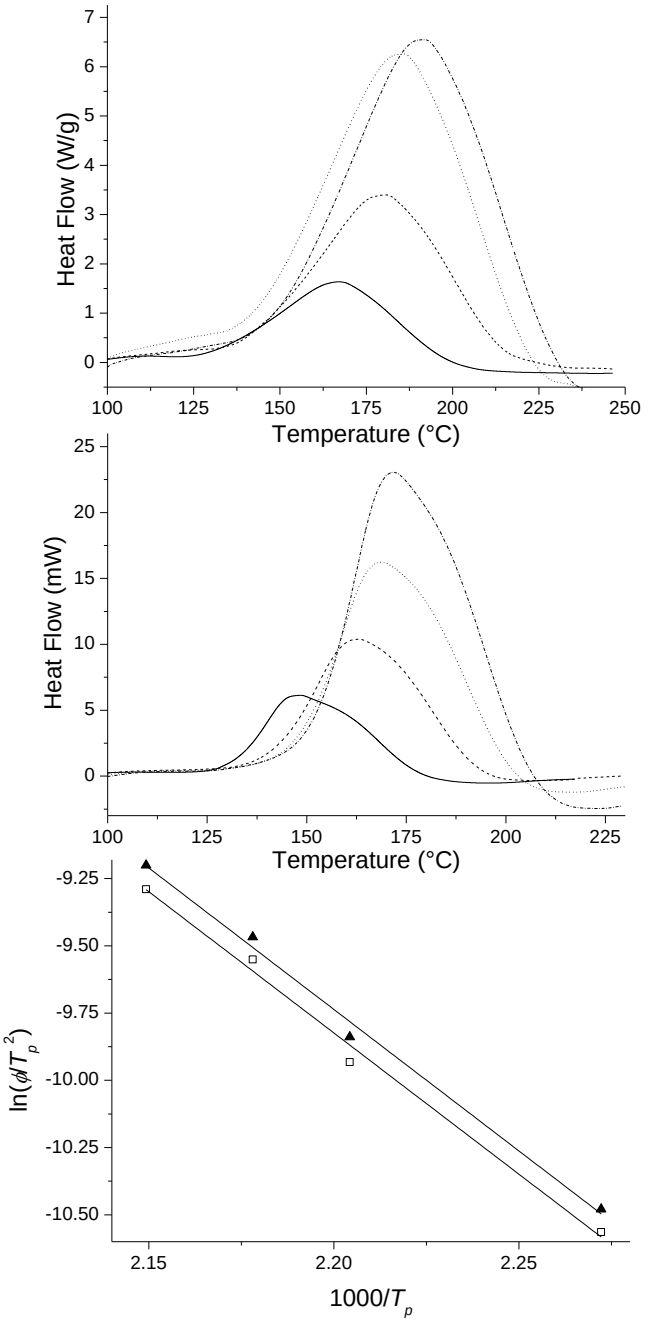

Figure 1. Evolution of DSC traces with temperature at heating rates of 5 °C min^{-1} (solid line), 10 °C min^{-1} (dashed line), 15 °C min^{-1} (dotted line), and 20 °C min^{-1} (dash–dotted line) during the cationic ROP of **5** (top) and **6** (middle) initiated by BzA–BF_3 (0.075 mol EE^{-1}). Corresponding Kissinger plots (bottom) for **5** (open squares) and **6** (solid triangles).

The activation energies (E_a) of the ROP of DET **5** and PEGDGE **6** initiated by BzA–BF_3 (0.075 mol EE^{-1}) were determined using the Kissinger method,[60] which is based on the assumption that the exothermic peak coincides with the maximum reaction rate as described by equation 6:

$$\ln\left(\frac{\phi}{T_p^2}\right) = \ln\left(\frac{k_0 R}{E_a}\right) - \left(\frac{E_a}{RT_p}\right) \quad (6)$$

with ϕ the heating rate, T_p the peak of the exothermal reaction and R the ideal gas constant. E_a and the frequency factors (k_0) of both reactive systems were obtained respectively from the slope and the origin of the linear relation of $\ln(\phi/T_p^2)$ as a function of T_p^{-1} (**Figure 1**). DSC scans performed from 25 to 250 °C at heating rates ranging from 5 to 20 °C min^{-1} exhibit very close activation energies for the ROP of epoxy monomers **5** and **6** (E_a = 87 and 85 kJ mol^{-1} respectively).

Table 1. DSC Data for Diepoxy Monomers 5, 6 and Epoxy Networks 7, 8 Obtained by Ring Opening Polymerization Initiated by BzA–BF_3 (0.075 mol EE^{-1}).

ENs	T_{g0} (°C)	ΔC_{p0} (J g^{-1} K^{-1})	ΔH_∞ (kJ EE^{-1})	$T_{g\infty}$ (°C)	$\Delta C_{p\infty}$ (J g^{-1} K^{-1})
5, **7**	−59	0.1199	91	−32	0.1016
6, **8**	−71	0.1900	89	−50	0.1528

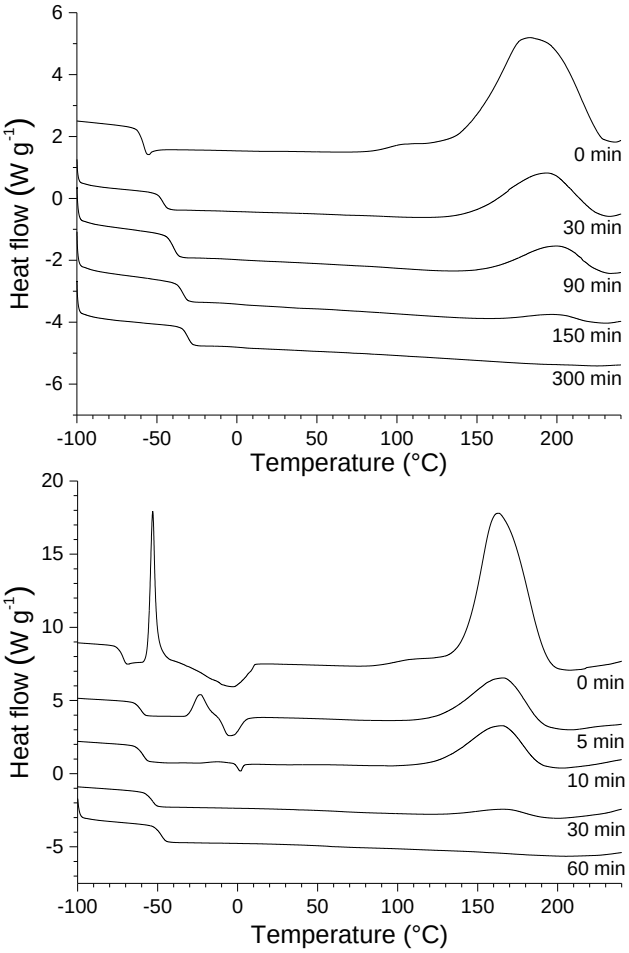

Figure 2. Evolution of DSC traces (heating rate = 10 °C min^{-1}) for the ROP of DET **5** (top) and PEGDGE **6** (bottom) initiated by BzA–BF_3 (0.075 mol EE^{-1}).

Kinetics of the Ring Opening Polymerization of Diepoxy Monomers 5 and 6. The ROP of DET **5** and PEGDGE **6** initiated by BzA–BF_3 (0.075 mol EE^{-1}) were initially compared by DSC monitoring. Typically, a first heating scan of the reactive mixtures was performed from –100 to 250 °C at a heating rate of 10 °C min^{-1} to determine T_{g0}, ΔC_{p0} and ΔH_∞ of each reactive system (**Figure 2** and **Table 1**). DET **5** is amorphous with a T_g of −59 °C while PEGDGE **6** is semi–crystalline with a glass transition (T_g = −71 °C), a cold crystallization transition (T_c = –53 °C) and a melting transition (T_m = −3 °C). Subsequently, initiation and propagation of the cationic ROP of DET **5** starts at ca. 85 °C and ends at ca. 230 °C while the peak of the exothermal reaction (T_p) is observed at 181 °C. In the case of PEGDGE **6** ROP starts at ca. 85 °C and ends at ca. 200 °C while T_p is located at 163 °C. Comparable T_p values have

been reported previously for the thermal curing of neutral diepoxy monomers initiated by BzA–BF_3.[45] Then, a second heating run from –100 to 250 °C of the cured sample afforded the final glass transition temperature ($T_{g\infty}$) and final differential heat capacity ($\Delta C_{p\infty}$) after full conversion of the reactive groups as confirmed by the disappearance of the exotherm corresponding to the ROP of epoxy groups. The enthalpies of reaction per equivalent epoxy are very close for the two epoxy monomers (ΔH_∞ = 91 and 89 kJ EE^{-1} for **5** and **6**, respectively) and on par with other reactive systems such as epoxies, cyanate–esters or bismaleimides for which ΔH_∞ is generally close to 90 kJ EE^{-1}.[54]

The kinetics of the cationic ROP of DET **5** and PEGDGE **6** initiated by BzA–BF_3 (0.075 mol EE^{-1}) at 130°C were then investigated by analyzing samples after different curing times by DSC (**Figure 2**) and by on–line FTIR monitoring of the decay of the absorption band of epoxy groups at 914 cm^{-1} during the curing (see e.g. **Figure S9** for DET **5**). The conversion of epoxy groups (x) calculated using equation 1 for DSC and equation 2 for FTIR was plotted as a function of time (t) in **Figure 3**. It is worth noting that a good agreement can be seen for kinetics results obtained using both monitoring methods. Complete conversions of epoxy groups were reached for curing times of ca. 300 min for DET **5** and 60 min for PEGDGE **6**. The ROP of DET **5** is thus significantly slower than the ROP of the neutral analogue PEGDGE **6**. As both systems show comparable activation energies, this difference most likely results from a probable ion exchange reaction. As previously pointed out,[61] initiation by an amine-BF_3 complex should proceed through decomposition of the latter into an ammonium tetrafluoroborate salt, which is in turn able to release the truly initiating species, i.e. the HBF_4 super-acid (**Scheme 3**). The ion exchange reaction between benzyl ammonium BF_3 and 1,2,3-triazolium TFSI enters in competition with the generation of HBF_4 and as a result slows down the process.

Scheme 3. Generation of HBF_4 Super-acid from the Amine-BF_3 Complex and Competitive Ion Exchange Reaction Between 1,2,3–Triazolium TFSI and the Benzyl Ammonium BF_4 Intermediate

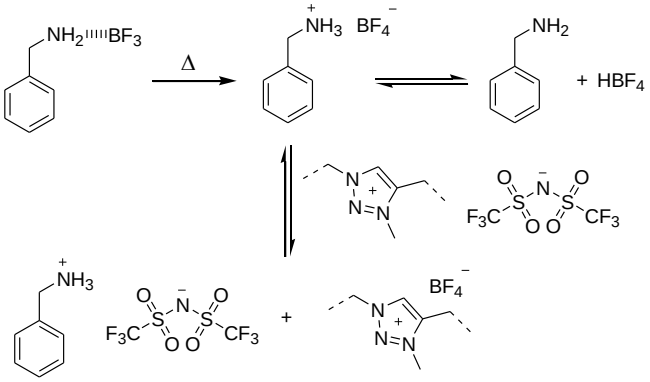

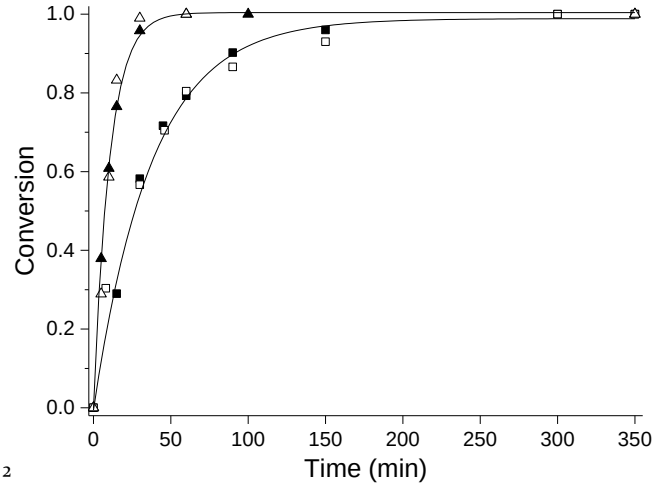

Figure 3. Evolution of conversion as a function of time for the ring opening polymerization at 130 °C initiated by BzA–BF_3 (0.075 mol EE^{-1}) of DET **5** (squares) and PEGDGE **6** (triangles) monitored by DSC (solid symbols) and FTIR (open symbols). Solid lines are guides to the eyes.

Monitoring of the Network Formation during the ROP of Diepoxy Monomers 5 and 6. The evolution of $T_g(t)$ as a function of x was monitored after an isothermal curing for a given time and subsequent DSC monitoring during a heating ramp from –100 °C to 200 °C to obtain $T_g(t)$ and $\Delta H(t)$ (**Figure 2**). The evolution of T_g as a function of x is described by equation (7):[47]

$$\frac{[T_g(t) - T_{g0}]}{[T_{g\infty} - T_{g0}]} = \frac{\lambda x}{[1-(1-\lambda)x]} \quad (7)$$

with $T_g(t)$ the glass transition temperature of the polymerization media after a curing time t (or a conversion x) and $\lambda = \Delta C_{p\infty}/\Delta C_{p0}$ (**Table 1**). Generally, $\lambda < 1$ for thermosetting polymers due to the inverse proportionality of ΔC_p with T_g, which is a necessary condition to obtain an upward curvature in the evolution of T_g with conversion.[63] As previously observed for other cross–linking reactions described for the synthesis of classical thermosetting polymers there is a fair agreement between experimental and theoretical evolutions of $T_g(t)$ with the conversion of epoxy groups for the ROP of DET **5** and PEGDGE **6** (**Figure 4**).[47] The high values of λ (0.847 and 0.804 for **5** and **6**) are representative of the low variation of T_g during the thermal curing which increases during the course of the ROP by 27 and 21 °C, respectively.

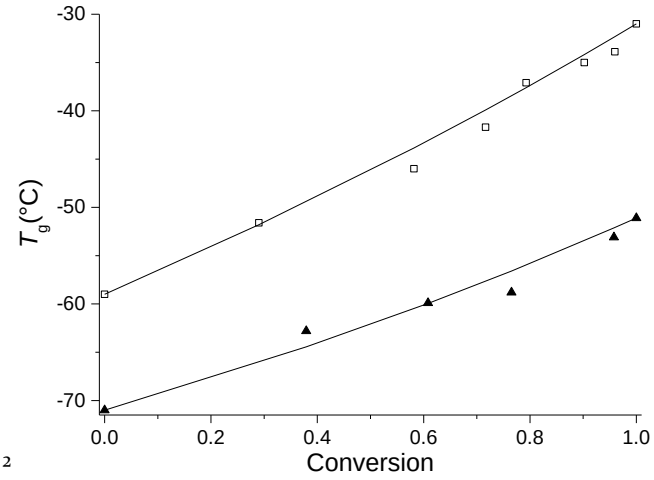

Figure 4. Evolution of T_g as a function of conversion during the ROP of **5** (open squares) and **6** (solid triangles) at 130 °C initiated by BzA–BF_3 (0.075 mol EE^{-1}). The solid lines are the theoretical predictions obtained from equation 7.

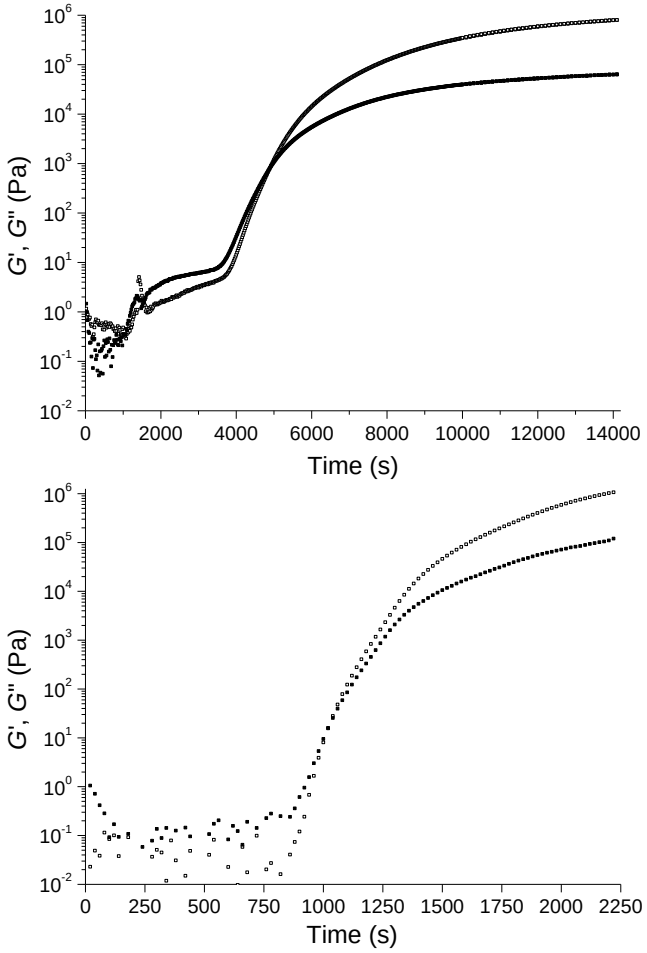

Figure 5. Evolution of the storage (*G*', solid squares) and loss (*G*", open squares) moduli during the ROP of DET **5** (top) and PEGDGE **6** (bottom) at 130 °C initiated by BzA–BF_3 (0.075 mol EE^{-1}).

The gelation behavior during the formation of epoxy networks **7** and **8** was investigated by rheological measurements. The gelation times (t_{gel}) at 130 °C during the cationic ROP of DET **5** and PEGDGE **6** at 130 °C initiated by BzA–BF_3 (0.075 mol EE^{-1}) were estimated by the crossover of *G*' and *G*" for a frequency of 1 rad s^{-1} (**Figure 5**). The conversions at the gel point (x_{gel}) were then calculated from the DSC measurements of the residual reaction enthalpy $\Delta H(t)$ for samples quenched in liquid nitrogen after an isothermal curing at 130 °C for $t = t_{gel}$ and using equation 1. The ROP of DET **5** exhibits higher t_{gel} and x_{gel} (x_{gel} = 83 %, t_{gel} = 4480 s) than PEGDGE **6** (x_{gel} = 72 %, t_{gel} = 1020 s). Typically for DGEBA homopolymerization, x_{gel} ranges from 5% to 20% when the activated chain end (ACE) mechanism is dominant i.e. whenever the cationic ROP is performed in absence of hydroxyl groups. Higher values (25

to 45%) are observed when the activated monomer (AM) mechanism is dominant, i.e. when hydroxides, other protic additives or impurities (water) are present.[45,52,54] The high x_{gel} values recorded here strongly suggest that the polymerization mechanism involves a significant amount of transfer and termination reactions. This most likely results from the presence of water traces (0.5 and 1.4 wt% representing 0.1 and 0.2 mol EE^{-1} for DET **5** and PEGDGE **6**, respectively) as measured by Karl–Fischer method. Besides the elevated curing temperature used herein, proton donating species such as water are known to provide transfer and termination reactions during cationic ROP. Moreover, it has been shown that the introduction of PEGDGE afforded a significant increase of t_{gel} and x_{gel} for the ROP of DGEBA initiated by 4CA–BF_3 (i.e. x_{gel} increases from 7% to 16% and t_{gel} increases from 2 to 13 min when 0.06 mol EE^{-1} of PEGDGE are added to DGEBA).[44] This can be explained by the ability of the PEG ether groups to form complexes with the initiator thus decreasing its efficiency. However as this phenomenon seems to be more important for the polymerization of DET **5** while its water content is ca. a third than for PEGDGE **6**, the previously mentioned ion metathesis reaction (**Scheme 3**) must have also an impact on the initiator efficiency and enhanced occurrence of transfer and termination reaction.

Table 2. Physical Properties of Epoxy Networks 7 and 8

	T_{d10}[a] (°C)	T_g[b] (°C)	T_α[c] (°C)	E'[c] (MPa)	S[d]	X[d] (%)	σ_{DC}[e] (S cm^{-1})
7	305	−32	−19	0.12	9.0	32.7	1.3×10^{-6}
8	330	−50	−37	0.75	2.7	16.6	4.6×10^{-7}

[a]: Obtained by TGA. [b]: Obtained by DSC. [c]: Obtained by rheology. [d]: Obtained by swelling experiments in acetone. [e]: Obtained by BDS at 30 °C under anhydrous conditions.

Physical and Thermomechanical Properties of Epoxy Networks 7 and 8. Based on polymerization kinetics studies, epoxy networks **7** and **8** were prepared in bulk by the cationic ROP of DET **5** and PEGDGE **6** initiated by BzA–BF_3 (0.075 mol EE^{-1}) carried out in silicone molds (V = 5.1 × 2.3 × 1.3 cm^3) and sequential curing under vacuum for 2 h at 100 °C, 8 h at 130 °C and 1 h at 150 °C. Thermal stability of epoxy networks **7** and **8** was first investigated by thermogravimetric analysis (**Figure S10**). Neutral epoxy network **8** exhibits a higher 10% weight loss temperature (T_{d10}) compared to ionic epoxy network **7** (T_{d10} = 330 and 305 °C, respectively). It is worth noting that while 1,2,3–triazolium units are often the weakest part regarding thermal stability of TPIL, T_{d10} of **7** is only slightly lower than **8**. T_{d10} of **7** corresponds to the upper range of values previously reported for TFSI–containing TPILs (T_{d10} ranges from 203 to 371 °C),[3] while it is comparable to 1,2,3–triazolium–based epoxy–amine network (T_{d10} = 308 °C).[46] Measurements of the swelling ratio (S) and amount of extractibles (X) is an easy and convenient method to qualitatively compare the structure and cross–link density of polymer networks (**Table 2**). Such measurements performed in acetone have shown that ionic epoxy network **7** swells significantly more than neutral epoxy network **8** (S = 9.0 and 2.7, respectively) and therefore the amount of extractibles of ionic epoxy network **7** is logically higher than the one of neutral epoxy network **8** (X = 32.7 % and 16.6 %, respectively). ^{1}H NMR of dried extractibles (results not shown) show that they mainly contain branched structures without any residual epoxy groups (**Figure S11**). These results corroborate earlier observations on the conversion at the gel point and further demonstrate that, due to the enhanced occurrence of transfer and termination reactions **7** has a lower cross–link density than **8**.

The thermomechanical properties of epoxy networks **7** and **8** were investigated by rheological temperature sweeps in torsion mode (**Figure 6** and **Table 2**). For both epoxy networks the alpha transition temperature (T_α) chosen as the maximum of the loss factor (tan(δ)) is 13 °C higher than T_g determined by DSC. However, ionic epoxy network **7** exhibits a significantly broader peak of tan(δ) ranging from −50 °C to 30 °C than neutral epoxy network **8** which ranges from −60 °C to 0 °C. This can most probably be explained by the plasticizing effect of the different quantities of low molar mass

species contained in the extractibles of epoxy networks **7** and **8**. Besides, ionic epoxy network **7** exhibits a lower value of elastic modulus at the rubbery plateau than neutral epoxy network **8** (E' = 0.12 and 0.75 MPa at 100 °C, respectively). In perfect agreement with previous results (i.e. higher x_{gel}, S and X values), these observations corroborate the structure difference between epoxy networks **7** and **8**, with a more loosely cross–linked network structure for epoxy network **7** which contains more structural defects such as dangling chains and branched species with finite molar masses.

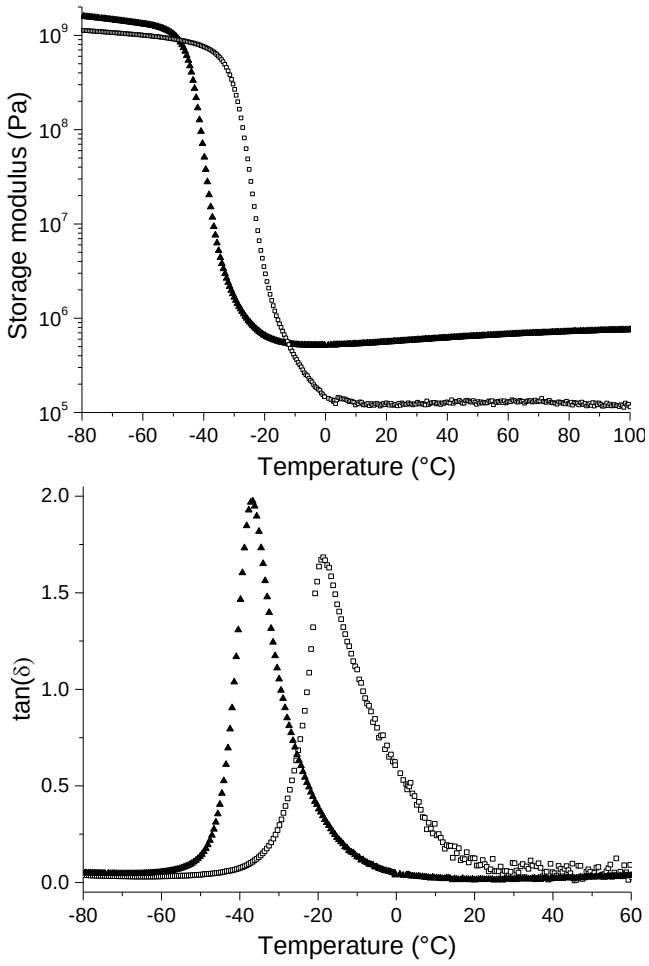

Figure 6. Evolution of storage moduli (a) and loss factors (b) as a function of temperature measured by torsional rheometry for epoxy networks **7** (open squares) and **8** (solid triangles).

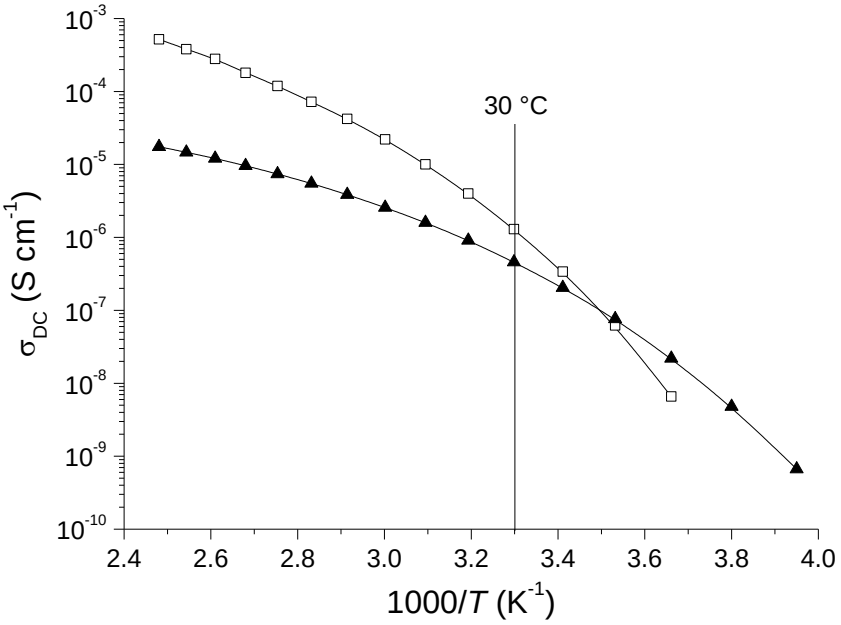

Figure 7. σ_{DC} versus reciprocal temperature measured by BDS for epoxy networks **7** (open squares) and **8** (solid triangles). The solid lines represent the best VFT fits of experimental data using equation 8 with σ_∞ = 0.12 S cm^{-1}, B = 1035 K, T_0 = 211 K for **7** and $\sigma_\infty = 8.4 \times 10^{-4}$ S cm^{-1}, B = 795 K, T_0 = 196 K for **8**.

Ion Conducting Properties of Epoxy Networks 7 and 8. The temperature dependence of the anhydrous ionic conductivity of epoxy networks **7** and **8** sandwiched between two platinum electrodes was investigated by broadband dielectric spectroscopy (**Figure S12**). For all samples, the dependence of of σ_{DC} on the reciprocal temperature above T_g follows a typical Vogel–Fulcher–Tammann (VFT) behavior (**Figure 7**) and experimental results were fitted with the VFT equation 8:

$$\sigma_{DC} = \sigma_\infty \times \exp\left(-\frac{B}{(T-T_0)}\right) \quad (8)$$

with σ_∞ the ionic conductivity in the limit of high temperatures, B the fitting parameter related to the activation energy of the ionic conduction, and T_0 the Vogel temperature. The ionic conductivity at 30 °C under anhydrous conditions of ionic epoxy network **7** ($\sigma_{DC} = 1.3 \times 10^{-6}$ S cm^{-1}) is higher than neutral epoxy network **8** ($\sigma_{DC} = 4.6 \times 10^{-7}$ S cm^{-1}) and is in the upper range of values previously reported for 1,2,3–triazolium–based networks with comparable T_g values (anhydrous σ_{DC} at 30 °C ranging from 2.2 $\times 10^{-11}$ to 1.0 $\times 10^{-6}$ S cm^{-1}).[3,40,47,63,64] The conductivity difference is even higher at high temperatures

as a result of the higher *B* parameter for **7**. This higher ionic conductivity may result from the high solubility, dissociation, and mobility of the TFSI counter–anion promoted by the low T_g flexible segments of the polymer network as well as the presence of numerous ether functionalities. Furthermore, the presence of charged macromolecular species of finite size resulting from transfer reactions could also play an important role. Besides, the lower cross–link density and the large amount of soluble fraction may also enhance the mobility of charge carriers and contribute to the higher ionic conductivity of epoxy network **7**. However, anhydrous ionic conductivity of epoxy network **8** is surprisingly high for a neutral polymer material and the higher ionic conductivity of **8** compared to **7** below room temperature is even more intriguing. This might be due to the lower T_g of the neutral epoxy network **8** compared to ionic epoxy network **7**. However, the significant concentration of ionic species resulting from the dismutation/hydrolysis of the Lewis acid initiator (ca. 1.9×10^{-4} mol cm^{-3}) may also contribute to this high value of σ_{DC} (**Scheme 3**). Although being lower than the concentration of 1,2,3–triazolium TFSI ion pairs (ca. 1.3×10^{-3} mol cm^{-3}) the much higher mobility of species issued from the initiator might contribute significantly to the ionic conductivity of epoxy network **7** and be the determining parameter for the ionic conductivity of epoxy network **8**.

CONCLUSIONS

In conclusion, we reported an original and straightforward synthetic pathway towards monocomponent cross–linked ion conducting networks. In contrast to previous reports based on diepoxy ILMs and diamine hardeners,[46,50,51] we showed here that the bulk cationic ring opening homopolymerization of a liquid diepoxy 1,2,3-triazolium ILM (i.e. DET **5)** readily affords PIL networks without using a comonomer which fatally dilutes the ionic species. The cationic ROP of DET **5** was investigating using a high pK_a amine/trifluoroborate complex (i.e. BzA–BF_3) initiator and compared to the ROP of a neutral analogue (i.e. PEGDGE **6**) to understand the impact of the ionic moiety on polymerization kinetics as well as on physical and thermomechanical properties of the resulting epoxy networks. The study of the

thermal curing behavior of these two monomers and the physical properties of the corresponding networks suggest that the ionic center affects the mechanism of polymerization and the structure of the network. Although PEGDGE **6** water uptake is higher than that of DET **5**, the ROP of the ionic system is slower than the neutral system. Besides, it seems that the 1,2,3–triazolium TFSI ion pairs might interact with the initiator thus reducing its efficiency and favoring the occurrence of transfer and termination reactions. These observations are in good agreement with swelling, extractibles and thermomechanical measurements. Indeed, higher swelling ratios, amounts of extractibles and conversions at the gel point together with a broader tan(δ) peak are observed for ionic epoxy network **7** indicating a less cross–linked network structure with more structural defects (i.e. dangling chains and branched species with finite molar masses) than for neutral epoxy network **8**. Nevertheless, the ionic system reaches quantitative conversion of epoxy groups and the corresponding network exhibit good thermal stability (T_{d10} = 304 °C) as well as remarkably high anhydrous ionic conductivity (σ_{DC} = 1.3 × 10^{-6} S cm^{-1} at 30 °C) for a cross-linked PIL. The assets of the resulting materials in combination with the desirable attributes of the cationic ROP process (i.e. prevention of hydroxide formation, a source of spurious protonic conduction and deleterious reactions with common electrolyte salts based on $LiPF_6$,[65] absence of network shrinkage and self-powered process by the exothermicity of the reaction) makes the proposed methodology of great interest for the conception of ion conducting polymer networks.

ASSOCIATED CONTENT

Supporting Information

The Supporting Information is available free of charge on the ACS Publications website at DOI: 10.1021/acs.macromol.XXXXX.

^{1}H and ^{13}C NMR of **2**, **3** and **5**, structures of initiators, DSC traces with temperature crude DET **5** and purified DET **5,** DSC traces with temperature of DET **5** in the presence of 0.075 mol EE^{-1} 2–PI, 1–MI, 4CA–BF_3 and BzA–BF_3, DSC traces with temperature of DET **5** and PEGDGE **6** initiated by BzA–BF_3

(0.075 mol EE^{-1}), DSC traces with temperature of epoxy networks **7** and **8,** On–line ATR–FTIR monitoring of the cationic ROP of DET **5** at 130 °C initiated by BzA–BF_3 (0.075 mol EE^{-1}), TGA traces of **7** and **8** (PDF).

AUTHOR INFORMATION

Corresponding Author

* (E.D.) E–mail: eric.drockenmuller@univ-lyon1.fr

ORCID

Antoine Jourdain: 0000-0002-6366-3958

Mona M. Obadia: 0000-0001-7613-3342

Anatoli Serghei: 0000-0002-6656-850X

Jannick Duchet-Rumeau: 0000-0002-1397-1434

Julien Bernard: 0000-0002-9969-1686

François Tournilhac: 0000-0002-6775-1584

Jean-Pierre Pascault: 0000-0001-6209-9040

Eric Drockenmuller: 0000-0003-0575-279X

Notes

The authors declare no competing financial interest.

ACKNOWLEDGMENTS

The authors gratefully acknowledge the financial support from the ANR through the MATVIT project (ANR-18-CE06-0026-01) and from the GDR LIPS CNRS #3585. We are grateful to T. Vidil for helpful discussions and advices. We thank M. Cloître and A. Guimet for their help in rheology monitoring experiments.

REFERENCES

(1) Yuan, J.; Mecerreyes, D.; Antonietti, M. Poly(ionic liquid)s : an update. *Prog. Polym. Sci*. **2013**, *38*, 1009–1036.

(2) Kohno, Y.; Saita, S.; Men, Y.; Yuan, J.; Ohno, H. Thermoresponsive polyelectrolytes derived from ionic liquids. *Polym.Chem.* **2015**, *6*, 2163–2178.

(3) Obadia, M. M.; Drockenmuller, E. Poly(1,2,3–triazolium)s: a new class of functional polymer electrolytes. *Chem. Commun*. **2016**, *52*, 2433–2450.

(4) Qian, W.; Texter, J.; Yan, F. Frontiers in poly(ionic liquid)s: syntheses and applications. *Chem. Soc. Rev*. **2016**, *46*, 1124–1159.

(5) Men, Y.; Kuzmicz D.; Yuan, J. Poly(ionic liquid)s colloidal particules. *Curr. Opin. Colloid Interface Sci*. **2014**, *19*, 76–83.

(6) Shaplov, A. S.; Ponkratov, D. O.; Vygodskii, Y. S. Poly(ionic liquid)s: Syntheis, Properties, and Applications. *Polym. Sci. Ser. B* **2016**, *2*, 73–142.

(7) He, H.; Rahimi, K.; Zhong, M.; Mourran, A.; Luebke, D. R.; Nulwala, H. B.; Möller M.; Matyjaszewski, K. Cubosomes from hierachical self–assembly of poly(ionic liquid) block copolymers. *Nat. Commun*. **2017**, *8*, 14057.

(8) Cordella, D.; Ouhib, F., Aqil, A.; Defiz, T.; Jérôme, C.; Serghei, A.; Drockenmuller, E.; Aissou, K.; Taton D.; Detrembleur, C. Fluorinated Poly(ionic liquid) Diblock Copolymers Obtained by Cobalt–Mediated Radical Polymerization–Induced Self–Assembly. *ACS Macro Lett*. **2017**, *6*, 121–126.

(9) Colliat-Dangus, G., Obadia, M. M.; Vygodskii, Y. S.; Serghei, A.; Shaplov, A. S.; Drockenmuller, E. Unconventional poly(ionic liquid)s combining motionless main chain 1,2,3–triazolium cations and high ionic conductivity. *Polym. Chem*. **2015**, *6*, 4299–4308.

(10) Wu, J.; Chen, J.; Wang, J.; Liao, X.; Xie, M.; Sun, R. Synthesis and conductivity of hyperbranched poly(triazolium)s with various end–capping groups. *Polym. Chem*. **2016**, *7*, 633–642.

(11) Tejero, R.; López, D.; López-Fabal, F.; Gómez-Garcés J. L.; Fernández-García, M. Antimicrobial

polymethacrylates based on quaternized 1,3–thiazole and 1,2,3–triazole side–chain groups. *Polym. Chem*. **2015**, *6*, 3449–3459.

(12) Elloumi, A. K.; Miladi, I. A.; Serghei, A.; Taton, D.; Aissou, K.; Ben Romdhane, H.; Drockenmuller, E. Partially Biosourced Poly (1,2,3–triazolium)–Based Diblock Copolymers Derived from Levulinic Acid. *Macromolecules*. **2018**, *51*, 5820–5830.

(13) Obadia, M. M.; Mudraboyina, B. P.; Serghei, A.; Phan, T. N. T.; Gigmes, D.; Drockenmuller, E. Enhancing Properties of Anionic Poly(ionic liquid)s with 1,2,3–Triazolium Counter Cations. *ACS Macro. Lett.* **2014**, *3*, 658–662.

(14) Obadia, M. M.; Colliat-Dangus, G.; Debuigne, A.; Serghei, A.; Detrembleur, C.; Drockenmuller, E. Poly(vinyl ester 1,2,3–triazolium)s: a new member of the poly(ionic liquid)s family. *Chem. Commun*. **2015**, *51*, 3332–3335.

(15) Adzima, B. J.; Taylor, S. C.; He, H.; Luebke, D. R.; Matyjaszewski K.; Nulwala, H. B. Vinyl-Triazolium Monomers: Versatile and New Class of Radically Polymerizable Ionic Monomers. *J. Polym. Sci. Part A: Polym. Chem*. **2014**, *52*, 417–423.

(16) Obadia, M. M.; Jourdain, A.; Serghei, A.; Ikeda, T.; Drockenmuller, E. Cationic and dicationic 1,2,3–triazolium–based poly(ethylene glycol ionic liquid)s. *Polym. Chem*. **2017**, *8*, 910–917.

(17) Liu, L.; He, S.; Zhang, S.; Zhang, M.; Guiver M. D.; Li, N. 1,2,3–Triazolium–Based Poly(2,6–Dimethyl Phenylene Oxide) Copolymers as Anion Exchange Membranes. *ACS Appl. Mater. Interfaces*. **2016**, *8*, 4651–4660.

(18) Jourdain, A.; Antoniuk, I.; Serghei, A.; Espuche, E.; Drockenmuller, E. 1,2,3–Triazolium–based linear ionic polyurethanes. *Polym. Chem.* **2017**, *8*, 5148–5156.

(19) Secker, C.; Robinson, J. W.; Schlaad, H. Alkyne–X modification of polypeptoids. *Eur. Polym. J.* **2015**, *62*, 394–399.

(20) Jourdain, A.; Serghei, A.; Drockenmuller, E. Enhanced Ionic Conductivity of a 1,2,3–Triazolium–Based Poly(siloxane ionic liquid) Homopolymer. *ACS Macro Lett*. **2016**, *5*, 1283–1286.

(21) Coupillaud, P.; Vignolle, J.; Mecerreyes, D.; Taton, D. Post–polymerization modification and organocatalysis using reactive statistical poly(ionic liquid)–based copolymers. *Polymer*. **2014**, *55*, 3404–3414.

(22) Zhou, X.; Weber, J.; Yuan, J. Poly(ionic liquid)s: platform for CO_2 capture and catalysis. *Curr. Opin. Green Sust. Chem*. **2019**, *16*, 39–46.

(23) Lee, C.-P.; Ho, K.-C. Poly(ionic liquid)s for dye–sensitized solar cells: A mini–review. *Eur. Polym. J.* **2018**, *108*, 420–428.

(24) Shaplov, A. S.; Ponkratov, D. O.; Aubert, P.-H.; Lozinskaya, E. I.; Plesse, C.; Vidal, F.; Vygodskii, Y. S. A first truly all–solid state organic electrochromic device based on polymeric ionic liquids. *Chem. Commun.* **2014**, *50*, 3191–3193.

(25) Puguan, J. M. C.; Jadhav, A. R.; Boton, L. B.; Kim, H. Fast–switching all–solid state electrochromic device having main–chain 1,2,3–triazolium–based polyelectrolyte with extended oxyethylene spacer obtained via click chemistry. *Sol. Energ. Mat. Sol. C* **2018**, *179*, 409–416.

(26) Zulfiqar, S.; Sarwar, M. I.; Mecerreyes, D. Polymeric ionic liquids for CO_2 capture and separation: potential, progress and challenges. *Polym. Chem*. **2015**, *6*, 6435–6451.

(27) Tomé, L. C.; Marrucho, I. Ionic liquid–based materials: a platform to design engineered CO_2 separation membranes. *Chem. Soc. Rev*. **2016**, *45*, 2785–2824.

(28) Muñoz-Bonilla, A.; Fernández-García, M. Poly(ionic liquid)s as antimicrobial materials. *Eur. Polym. J.* **2018**, *105*, 135–149.

(29) Gao, R.; Wang, D.; Heflin, J. R.; Long, T. E. Imidazolium sulfonate–containing pentablock copolymer–ionic liquid membranes for electroactive actuators. *J. Mater. Chem*. **2012**, *22*, 13473–13476.

(30) Guterman, R.; Ambrogi, M.; Yuan, J. Harnessing Poly(ionic liquid)s for Sensing Application. *Macromol. Rapid Commun.* **2016**, *37*, 1106–1115.

(31) Choi, J.-H.; Xie, W.; Gu, Y.; Frisbie, C. D.; Lodge, T. P. Single Ion Conducting, Polymerized Ionic Liquid Triblock Copolymer Films: High Capacitance Electrolyte Gates for n–type Transistors. *ACS*

Appl. Mater. Interfaces. **2015**, *7*, 7294–7302.

(32) Díaz, M.; Ortiz, A.; Ortiz, I. Progress in the use of ionic liquids as electrolyte membranes in fuel cells. *J. Membrane Sci.* **2014**, *469*, 379–396.

(33) Shaplov, A. S.; Marcilla, R.; Mecerreyes, D. Recent advances in innovative polymer electrolytes based on poly(ionic liquid)s. *Electrochim. Acta.* **2015**, *175*, 18–34.

(34) Ponkratov, D. O.; Lozinskaya, E. I.; Vlasov, P. S.; Aubert, P.-H.; Plesse, C.; Vidal, F.; Vygogskii, Y. S.; Shaplov, A. S. Synthesis of novel families of conductive cationic poly(ionic liquid)s and their application in all–polymer flexible pseudo–supercapacitors. *Electrochim. Acta.* **2018**, *281*, 777–788.

(35) Ajjan, F. N.; Ambrogi, M.; Tiruye, G. A.; Cordella, D.; Fernandes, A. M.; Grygiel, K.; Isik, M.; Patil, N.; Porcarelli, L.; Rocasalbas, G.; Vendramientto, G.; Zeglio, E.; Antonietti, M.; Mecerreyes, D.; Moreno, M.; Taton, D.; Solin, N.; Yuan, J. Innovative Polyelectrolytes/Poly(ionic liquid)s for energy and Environment. *Polym. Int.* **2017**, *66*, 1119–1128.

(36) Eshetu, G. G.; Mecerreyes, D.; Forsyth, M.; Zhang, H.; Armand, M. Polymeric ionic liquids for lithium–based rechargeable batteries. *Mol. Syst. Des. Eng.* **2019**, *4*, 294–309.

(37) Alesanco, Y.; Viñuales, A.; Rodriguez, J.; Tena-Zaera, R. All–in–one gel–based electrochromic devices: Strengths and recent developments. *Materials.* **2018**, *11*, 414.

(38) Wilke, A.; Yuan, J.; Antonietti, M.; Weber, J. Enhanced carbon dioxide adsorption by a mesoporous poly(ionic liquid). *ACS Macro Lett.* **2012**, *1*, 1028–1031.

(39) Guo, J.; Xu, Q.; Zheng, Z.; Zhou, S.; Mao, H.; Wang, B.; Yan, F. Intrinsically Antibacterial Poly(ionic liquid) Membranes: The Synergistic Effect of Anions. *ACS Macro. Lett.* **2015**, *4*, 1094–1098.

(40) Tracy, C. A.; Adler, A. M.; Nguyen, A.; Johnson, R. D.; Miller, K. M. Covalently Crosslinked 1,2,3–Triazolium–Containing Polyester Networks: Thermal, Mechanical, and Conductive Properties. *ACS Omega.* **2018**, *3*, 13442–13453.

(41) Carlisle, T. K.; McDanel, W. M.; Cowan, M. G.; Noble, R. D.; Gin, D. L. Vinyl–functionalized poly(imidazolium)s: a curable polymer platform for cross–linked ionic liquid gel synthesis. *Chem.*

Mater. **2014**. *26*, 1294–1296.

(42) Champagne, P.-L.; Ester, D.; Zeeman, M.; Zellman, C.; Williams, V. E.; Ling, C.-C. Inverting Substitution Patterns on Amphiphilic Cyclodextrins Induces Unprecedented Formation of Hexagonal Columnar Superstructures. *J. Mat. Chem. C*. **2017**, *5*, 9247–9254.

(43) Knapp, D. C.; D'Onofrio, J.; Engels, J. W. Fluorescent Labeling of (Oligo)Nucleotides by a New Fluoride Cleavable Linker Capable of Versatile Attachment Modes. *Bioconjugate Chem.* **2010**, *21*, 1043–1055.

(44) Vidil, T.; Tournilhac, F. Supramolecular Control of Propagation in Cationic Polymerization of Room Temperature Curable Epoxy Compositions. *Macromolecules*. **2013**, *46*, 9240–9248.

(45) Bouillon, N.; Pascault, J.-P.; Tighzert, L. Epoxy prepolymers cured with boron trifluoride–amine complexes, 1: Influence of the amine on the curing window. *Makromol. Chem.* **1990**, *191*, 1403–1416.

(46) Nguyen, T. K. L.; Obadia, M. M.; Serghei, A.; Livi, S.; Duchet-Rumeau, J.; Drockenmuller, E. 1,2,3–Triazolium–Based Epoxy–Amine Networks: Ion–Conducting Polymer Electrolytes. *Macromol. Rapid Commun*. **2016**, *37*, 1168–1174.

(47) Pascault, J.-P.; Williams, R. J. J. *Epoxy Polymers: New materials and innovations,* Wiley–VCH, 2010, p 139, ISBN: 978-3-527-32480-4.

(48) Ligon, S. C.; Liska, R.; Stampfl, J.; Gurr, M.; Mülhaupt, R. Polymers for 3D Printing and Customized Additive Manufacturing. *Chem. Rev.* **2017**, *117,* 10212–10290.

(49) Matsumoto, K.; Endo, T. Design and Synthesis of ionic–conductive epoxy–based networked polymers. *React. Funct. Polym.* **2013**, *73*, 278–282.

(50) McDanel, W. M.; Cowan, M. G.; Barton, J. A.; Gin, D. L. Effect of Monomer Structure on Curing Behavior, CO2 Solubility, and Gas Permeability of Ionic Liquid–Based Epoxy–Amine Resins and Ion–Gels. *Ind. Eng. Chem. Res.* **2015**, *54*, 4396–4406.

(51) Livi, S.; Chardin, C.; Lins, L. C.; Halawani, N.; Pruvost, S.; Duchet-Rumeau, J.; Gérard, J.-F.; Baudoux, J. From Ionic Liquid Epoxy Monomer to Tunable Epoxy–Amine Network: Reaction

Mechanism and final properties. *ACS Sustainable Chem. Eng.* **2019**, *7*, 3602–3613.

(52) Vidil, T.; Tournilhac, F.; Musso, S.; Robisson, A.; Leibler L. Control of reactions and network structures of epoxy thermosets. *Progress Polym. Sci.* **2016**, *62*, 126–179.

(53) Heise, M. S.; Martin, G. C. Curing Mechanism and Thermal Properties of Epoxy–Imidazole Systems. *Macromolecules* **1989**, *22*, 99–104.

(54) Matejka, L.; Chabanne, P.; Tighzert, L.; Pascault, J.-P. Cationic Polymerization of Diglycidyl Ether of Bisphenol A. *J. Polym. Sci. Part A: Polym. Chem.* **1994**, *32*, 1447–1458.

(55) Vidil, T.; Cloître, M.; Tournilhac, F. Control of Gelation and Network Properties of Cationically Copolymerized Mono– and Diglycidyl Ethers. *Macromolecules* **2018**, *51*, 5121–5137.

(56) Kim, M. S.; Lee, K. W.; Endo, T.; Lee, S. B. Benzylpyrazinium Salts as Thermally Latent Initiators in the Polymerization of Glycidyl Phenyl Ether: Substituent Effect on the Initiator Activity and Mechanistic Aspects. *Macromolecules* **2004**, *37*, 5830–5834.

(57) Ryu, C. Y.; Spencer, M. J.; Crivello, J. V. Involvement of Supramolecular Complexes in the Capture and Release of Protonic Acids During the Cationic Ring–Opening Polymerization of Epoxides. *Macromolecules* **2012**, *45*, 2233–2241.

(58) Ooi, S. K.; Cook, W. D.; Simon, G. P.; Such, C. H. DSC studies of the curing mechanisms and kinetics of DGEBA using imidazole curing agents. *Polymer* **2000**, *41*, 3639–3649.

(59) Obadia, M. M.; Jourdain, A.; Cassagnau, P.; Montarnal, D.; Drockenmuller, E. Tuning the Viscosity Profile of Ionic Vitrimers Incorporating 1,2,3-Triazolium Cross-Links *Adv. Funct. Mater.* **2017**, *27*, 1703258.

(60) Salla, J. M.; Ramis, X. Comparative study of the cure kinetics of an unsaturated polyester resin using different procedures. *Polym. Eng. Sci.* **1996**, *36*, 835–851.

(61) Vidil, T.; Tournilhac, F.; Leibler, L. Control of cationic epoxy polymerization by supramolecular initiation. *Polym. Chem.* **2013**, *4* (5), 1323-1327.

(62) Pascault, J.-P.; Williams, R. J. J. Glass Transition Temperature Versus Conversion, Relationship

For Thermosetting Polymers. *J. Polym. Sci. Part B: Polym. Phys.* **1990**, *28*, 85–95.

(63) Abdelhedi-Miladi, I.; Montarnal, D.; Obadia, M. M.; Romdhane, H. B.; Drockenmuller, E. UV–Patterning of Ion Conducting Negative Tone Photoresists Using Azide–Functionalized Poly(Ionic Liquid)s. *ACS Macro. Lett.* **2014**, *3*, 1187–1190.

(64) Lopez, G.; Granado, L.; Coquil, G.; Larez-Sosa, A.; Louvain, N.; Améduri, B. Perfluoropolyether (PFPE)–Based Vitrimers with Ionic Conductivity. *Macromolecules* **2019**, *52*, 2148–2155.

(65) Xu, K. Nonaqueous Liquid Electrolytes for Lithium-Based Rechargeable Batteries. *Chem. Rev.* **2004**, *104* (10), 4303-4417

TOC graphic: